International Journal of Applied Earth Observations and Geoinformation 105 (2021) 102622

Contents lists available at ScienceDirect

International Journal of Applied Earth Observations and Geoinformation

journal homepage: www.elsevier.com/locate/jag

The naturalness index for the identification of natural areas on regional scale

Burak Ekim[a,1], Zeyu Dong[b,1], Dmitry Rashkovetsky[b], Michael Schmitt[a,*]

[a] Institute of Space Technology and Space Applications, Bundeswehr University Munich, Neubiberg, Germany
[b] Department of Aerospace and Geodesy, Technical University of Munich, Munich, Germany

ARTICLE INFO

Keywords:
Mapping
Conservation
Data Fusion
Naturalness
Earth Observation
Cloud Computing
Earth Engine

ABSTRACT

Researchers have been trying to measure the influence of humankind on our environment for several decades. Among the technical solutions for this goal, approaches for a rule-based fusion of different geospatial information layers have reached the greatest level of maturity, enabling the (semi-)automatic production of maps at resolutions of about 1 square kilometer. While those existing approaches aim at a global analysis of human influence, conservation efforts are usually implemented on a regional scale. To bridge the gap between a global, low-resolution analysis and a local, high-resolution analysis, with this paper, we propose the Naturalness Index (NI), which represents the naturalness of the Earth's surface as a metric between 0 and 100 at a spatial resolution of 10 m per pixel. Our approach builds on the established Human Influence Index, but replaces different geospatial input layers with more recent, higher resolution counterparts. Using the cloud computing platform Google Earth Engine, regional maps at a resolution of 10 m × 10 m per pixel can be produced efficiently in a fully automatic manner. We demonstrate the functionality by creating maps for three different localities in Europe – Bavaria, Lapland, and Scotland. A comparison of the NI values achieved with our approach to official conservation areas as well as a correlation with existing similar maps indicate the validity of our approach.

1. Introduction

Under the impression of the so-called Corona crisis, the World Health Organization (WHO) published the "WHO Manifesto for a healthy recovery from COVID-19" in May 2020 (WHO, 2020), which claimed that better global environmental protection can help to mitigate future risks for epidemic plagues. The reason for this is that many diseases have a zoonotic origin, and leaving wild animals alone in their natural habitats can prevent those diseases from being transferred to the human population. In order to protect natural habitats, the designation of conservation areas is in need. Besides that, researchers have also confirmed manifold ecological and even economic reasons for the conservation of nature (Potapov et al., 2017; Balmford et al., 2002).

However, especially in densely populated countries, taking land away from exploitation by business, traffic, agriculture or forestry does not go without opposition from the regional communities, who do not want to lose their land use rights. Often, the argument is that there is no real nature left anyway, and that exempting land from civilization would be an unjustified expropriation. With that in mind, it seems reasonable to objectify the determination of whether an area is "natural" or under strong human influence (see, e.g., Brackhane et al., 2021). One option to do so is by means of modern geospatial data analysis, as frequently done in the context of "wilderness" mapping (Carver et al., 2013; Carver & Fritz, 2016; Fritz et al., 2000; Cao et al., 2019; Ma & Long, 2020). Almost 20 years ago, Sanderson et al. (2002) proposed the human footprint, quantified by the human influence index (HII), to map how much human civilization has influenced the land surface. To calculate the HII, they relied on four types of geospatial input data:

- population density, expressed by population density grids
- land transformation, expressed by land use maps
- accessibility, expressed by the proximity to traffic ways
- electrical power infrastructure, expressed by nighttime lights

By rescaling all the globally available input data to a resolution of 1 km × 1 km and scaling each input source's contribution with a score between 0 (for the absence of human influence) and 10 (for high human influence), they created a map of the global human footprint. Some

* Corresponding author.
E-mail address: michael.schmitt@unibw.de (M. Schmitt).
[1] Authors contributed equally to this work.

https://doi.org/10.1016/j.jag.2021.102622
Received 16 June 2021; Received in revised form 6 November 2021; Accepted 10 November 2021
Available online 20 November 2021
0303-2434/

years later, Venter et al. (2016) used this approach to investigate the change of human influence between 1993 and 2009. In their study, they found that during this period, the human footprint has increased by 9%, with 75% of the Earth's land surface experiencing measurable human pressure. In a similar manner, Allan et al. (2017) published temporally intercomparable maps of terrestrial wildernesses. Since they defined wilderness areas as pressure-free lands with a contiguous area of more than 10,000 km^2, they found Europe to be void of any truly wild areas. The most recent research output in that direction is the 1 km^2-resolution Human Modification (HM) map published by Kennedy et al. (2019). This map provides a cumulative measure of human modification of terrestrial lands as a continuous measure ranging from 0 to 1. This score reflects the proportion of a landscape modified based on 13 anthropogenic stressors and their estimated impacts using spatially-explicit global datasets. The data is derived from the median year 2016.

In the work described in this paper, we do not focus on the identification of wilderness, nor a global analysis of changes in terms of large-scale wilderness areas. Instead, we intend to bridge the gap between a global, low-resolution analysis of human influence or modification on land masses and a regional, high-resolution mapping of its absence. For that purpose, we propose the naturalness index (NI) to quantify the amount of human influence/modification – or absence thereof – on the environment at a resolution of 10 m $\times$ 10 m. The basis of the NI is formed by an upscaling of the HII procedure to higher spatial resolutions with most recent data sources using automated, cloud-based computation in Google Earth Engine (Gorelick et al., 2017) as processing environment. While the earlier approaches put a clear focus on global mapping for a global understanding of human influence and nature degradation, our intention is to provide more fine-grained regional information to regional conservation stakeholders. With our results, the areas that can be considered most natural from a technical point of view in a state or country can be determined based on objective geospatial information. In summary, the contributions of this work are:

- We propose the new Naturalness Index metric, which improves the HII by introducing updated land transformation scores and a more sophisticated accessibility function, and includes a different scaling and normalization.
- We update the geodata sources used to calculate the HII in earlier literature by more recent sources equipped with more advanced methods and sensors with higher spatial resolution. While doing so, we make sure that those sources are available on an international scale to ensure reproducibility.
- We improve the measurement of land accessibility by combining distance from the nearest trafficway with topographic information using a geographical function.
- We implement the workflow in Google Earth Engine for fast, reproducible large-scale mapping.
- We produce naturalness maps for three different European regions: the German state of Bavaria as an example for a densely populated region (about 180 people per km^2) with only few and small designated conservation areas; Scotland as a region with medium population density (about 70 people per km^2) and a larger share of remote areas; and the Lapland region of Finland for a sparsely populated landscape (about 2 people per km^2) with an abundance of protected areas.
- We validate the NI by comparing the produced naturalness map with existing conservation areas.

The remainder of the paper is structured as follows: In Section 2, we describe our approach to create a Naturalness Index at a resolution of 10 m per pixel on a regional scale. In Section 3, we show results for three study areas, namely: Bavaria, Lapland, and Scotland. We argue that the study areas adopted in this study are characterized by different degrees of population density and human influence and thus provide a coherent test bed to demonstrate the global applicability of the developed approach. In the same section, we further provide a qualitative and quantitative analysis study of regional naturalness index maps including a comparison with similar indices. Section 4 contains a discussion of the results found in our study.

2. Calculation of the naturalness index

2.1. Overview of the approach

Fig. 1 shows a flowchart of the developed approach that extends the previous work of Sanderson et al. (2002) by further taking land cover penalty terms and accessibility measures into account to shape a more precise measure. Apart from these newly-introduced extensions, scale and inversion operations are applied to the recent geospatial data sources with higher resolutions to form a more informative NI. With this NI, we intend to measure the naturalness of the Earth's land surface from the perspective of absent human influence.

The approach presented in this work exploits four different geospatial data sources as proxies for naturalness: population density, land cover, accessibility, and electrical power infrastructure. Although these data sources are provided at high spatial resolution, provide global coverage, and are openly available, their ability to characterize naturalness individually is limited owing to their ambiguous nature. Thus, a rule-based geospatial data fusion has to be applied to construct an inclusive naturalness measure.

In order to do so, the four different data sources are first pre-processed and then re-classified or weighted, before they are added up to calculate an upscaled, modernized variant of the HII in a manner similar to the approach described by Sanderson et al. (2002). Then, the numbers are inversely scaled to the range [0;100]. While the original HII went from 0 (complete absence of human influence) to 72 (the theoretical maximum, strongest human influence), our *Naturalness Index* theoretically ranges from 0 (least natural state, strongest human influence) to 100 (most natural state, weakest human influence). Even though the theoretical range is [0;100], in practice (e.g. for visualization purposes) the range [0;80] is used. This is motivated by the observation that the NI values mostly reside far from the upper limit, given the lack of completely natural ("wilderness") areas in our developed world.

The different data sources used to form the NI are described in the following subsections, including the pre-processing and scaling applied to them.

2.2. Recent high-resolution geodata input

As in the initial work on the HII, four geospatial variables are needed as proxies for human influence, or – inversely – naturalness: population density, land transformation, accessibility, and electrical power infrastructure. We use sources that are as recent and as highly resolved as possible, while still being available freely on a global scale. The different sources are summarized and compared to the original sources in Table 1.

2.2.1. Population density

The density of the human population is considered as a main factor of destruction in the environment (Cincotta et al., 2000), thus forming an adequate measure for the absence of naturalness. In addition, the population density can be considered as a sign of need of resources which inherently degregates the surrounding environment.

Unfortunately, the only source for international geodata on population distribution is the Gridded Population of the world. However, this product provided by CIESIN is regularly updated and comes with a projection for the year 2020 in version 4.11. Although only available at a resolution of 30 arc seconds (approx. 926 m at the equator and 654 m at a latitude of 45°), population density is of course a crucial input to a mapping of human influence on land surfaces. We thus keep this input, although we suggest replacing it with a more high-resolution source should this become available in the future.

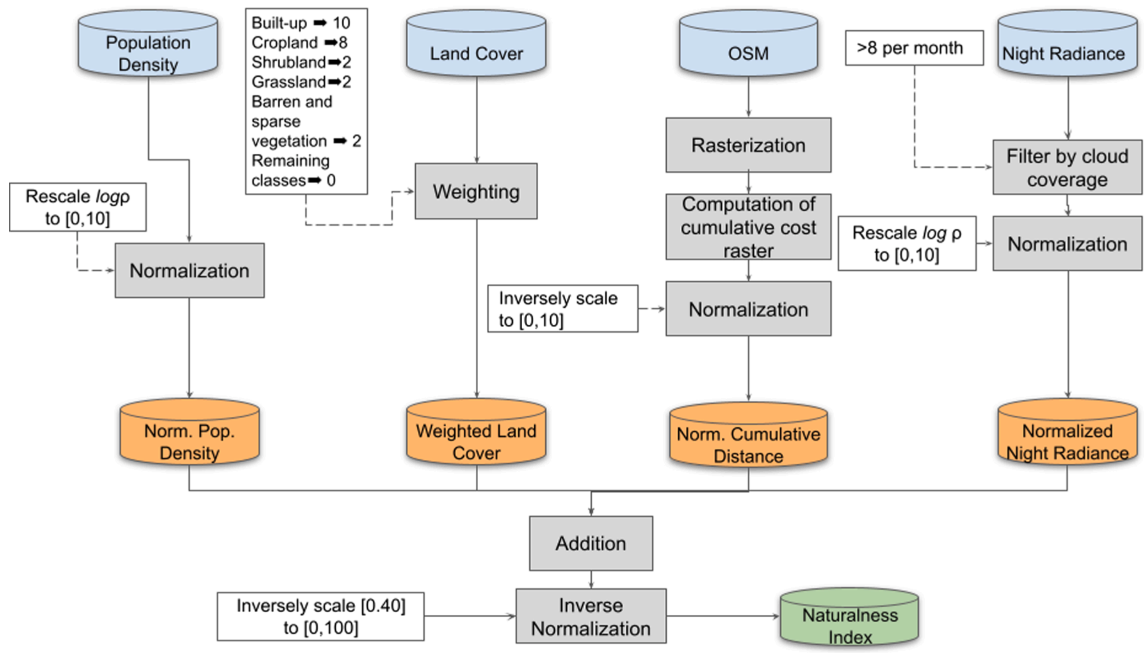

Fig. 1. Adapted workflow, implemented in Google Earth Engine.

Table 1
Geospatial data sources: HII versus NI.

Geospatial Data Source	Human Influence Index			Naturalness Index (Ours)		
	Dataset	Year	Resolution	Dataset	Year	Resolution
Population density	Gridded Population of the World v2	1995	2.5 arc minutes	Gridded Population of the World v4.11	2020	30 arc seconds
Land transformation	Global Land Use/Land Cover v2	1992–1993	1 km	WorldCover V100	2020	10 m
Accessibility	Vector Maps	1960–1990s	–	OpenStreetMap	2020	–
Electrical power infrastructure	Defense Meteorological Satellite Program Stable Lights	1994–1995	30 arc seconds	VIIRS Stray Light Corrected Nighttime Day/Night Band Composites Version 1	Monthly average from 2014 – present	15 arc seconds

In our approach, the population density is normalized with a threshold of 1000 persons per square kilometer. Any pixel where the density exceeds this threshold receives the maximum score of 10, otherwise the density values are min–max scaled to a range of [0;10] after logarithmic transformation.

2.2.2. *Land transformation*

In the earlier approaches, land cover data was used to model the transformation of natural land into cultivated landscapes. We follow this idea but stick closer to the meaning of classic land cover classes. The fact that, e.g., an urban area is not a form of natural land cover is as obvious as, e.g., forest areas representing a relatively natural class.

Since the resolution of land cover maps depends mostly on the remote sensing input data used to derive the land cover representations, significant progress was enabled in the last decades by the growing availability of freely available high-resolution satellite imagery. Thus, we replace the original global land use/land cover data with a resolution of 1 km by the WorldCover V100 data with a resolution of 10 m produced from Sentinel-1 and Sentinel-2 imagery by ESA (Zanaga et al., 2021). The conversion of WorldCover V100 land cover classes in weight factors is outlined in Fig. 1. Furthermore, the water class is masked out in the final result given the reason that large water bodies are often intensively used for fishing, water sports or tourism and generally enable access to their shores. They are thus exempted from our processing, which focuses on land surfaces only.

2.2.3. *Accessibility*

Apart from population density and land transformation, access to non-inhabited areas determines whether the human population can influence the land. Access is provided by roads, railways and navigable rivers. We make use of OpenStreetMap (OSM) data, as it is usually up-to-date and globally available, even though the quality is not homogeneous across the globe (Haklay, 2010). In order to deduce accessibility from OSM, we first rasterize the OSM *roads, railways, and waterways* vector layer into a GeoTIFF file with a resolution of 10 m. Then, we convert this raster to an accumulated cost surface encoding the cumulative cost to the nearest traffic way for every pixel. The cost to traverse each pixel, represented in minutes per meter, is determined by the walking pace based on terrain slope, calculated by Tobler's hiking function for off-path travel (Tobler, 1993). The prime source to calculate the terrain slope is the NASA Shuttle Radar Topography Mission (SRTM) Digital Elevation Model at a pixel spacing of 30 m. For the high latitude regions (>60°N or 56°S) residing outside the coverage of SRTM model, we replace it with the ALOS Global Digital Surface Model, which is also provided with a pixel spacing of 30 m. The maximum distance used for computation is 15 km. Finally, the cumulative costs are inversely scaled to a range of [0;10], with an upper threshold of eight hours as the maximum time limit a person can walk in one day. This process is illustrated in Fig. 2. An example of the maps produced from the workflow is provided in Fig. 3.

2.2.4. *Electrical power infrastructure*

A final proxy for the influence of humanity on the environment is the

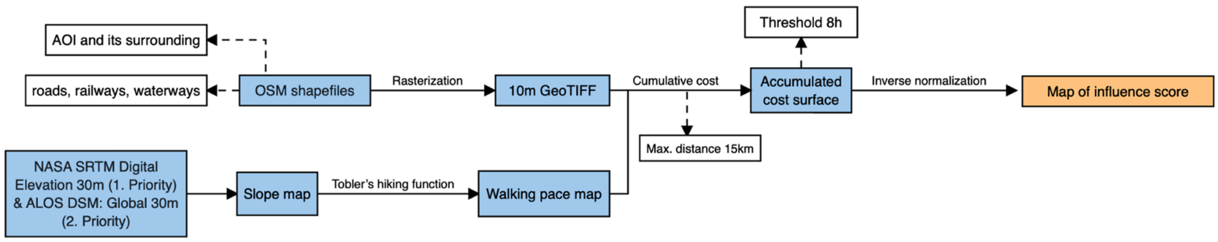

Fig. 2. Workflow to deduce accessibility.

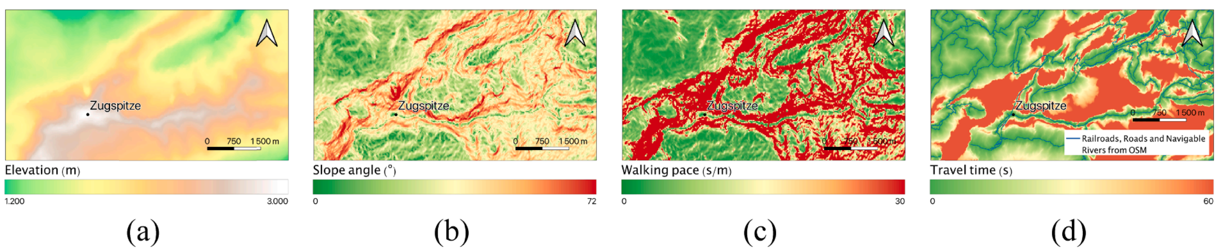

Fig. 3. An example image of (a) a digital elevation map (source: SRTM), (b) a slope map calculated from elevation, (c) a walking pace map based on terrain slope calculated using Tobler's hiking function for off-path travel, (d) and an accumulated cost surface calculated over 15 km maximum distance.

availability of electrical power, which can be approximated by analyzing nighttime illumination. Following the reasoning of Sanderson et al. (2002), we use monthly averaged VIIRS Stray Light Corrected Nighttime imagery and scale it in a similar manner as the population density, namely by normalization with a threshold and subsequent logarithmic transformation. The upper limit for the computation is 30 nanoWatts/cm2/sr. Although the resolution of the dataset is only 15 arc seconds (corresponding to 463 m at the equator and 327 m at a latitude of 45°), we still consider this input as an important piece of information, which should not be ignored.

2.3. *Converting the scores to the final naturalness index*

Once all four input datasets are converted to weights, these weights are summed up for every pixel, leading to our modernized and upscaled version of the HII. The resulting score is then inversely normalized to the range [0;100] in order to gain the desired Naturalness Index. Since larger water bodies are not properly represented by the calculation of HII or NI, respectively, we further mask them by setting all pixels corresponding to the Global Forest Change water mask of Hansen et al. (2013) to NaN values.

3. Example results and validation

In order to demonstrate and validate the feasibility of the Naturalness Index proposed in this work, we use the methodology described in Section 2 for the automatic production of NI maps for three different study areas: Bavaria, Lapland, and Scotland (see Fig. 4). These study areas were selected based on their different degrees of population density and are described in the following.

3.1. *Study areas*

Bavaria is a landlocked federal state of Germany, occupying an area of about 70,550 km^2. With a population density of 185 people per km^2 and eight cities with more than 100,000 inhabitants, it serves as a good example for a densely populated central European region. According to the Bavarian State Ministry of the Environment, about 3% of the state's area are designated conservation areas with strong protection status: two national parks and almost 600 less strictly protected nature reserves.

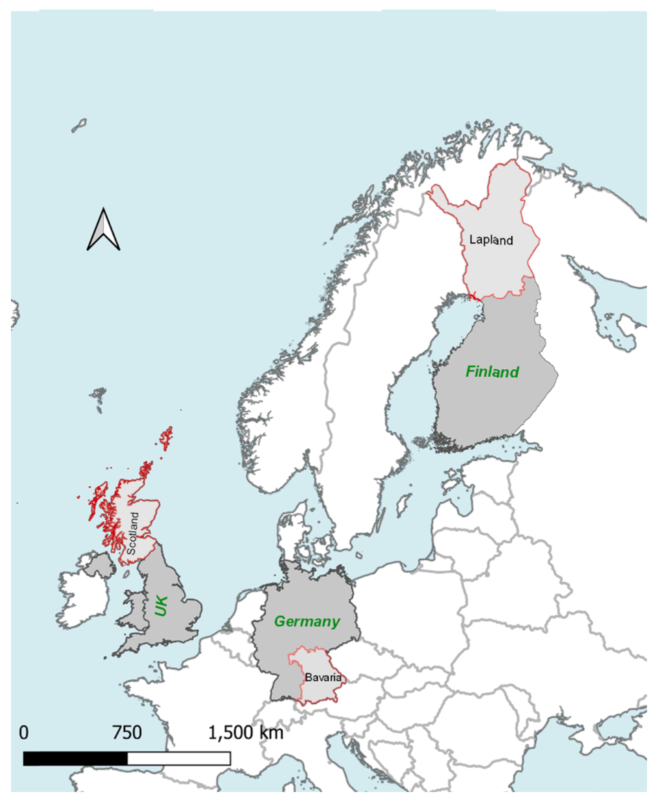

Fig. 4. Overview of the study areas: Bavaria, Lapland, and Scotland.

Lapland is the largest and northernmost region of Finland and covers a land area of 92,667 km^2 plus an additional 6316 km^2 of lakes and rivers. With a landscape mainly consisting of mires and forests in the South and fells in the North, it is one of the least populated regions in Europe – only about 2 people per km^2 live there. With more than 900 designated conservation areas in total, almost all of Lapland (about 90,000 km^2) is protected. Thus, in this study, Lapland serves as a good example for a sparsely populated region at the (sub-)arctic outskirts of Europe.

Finally, **Scotland** is supposed to serve as an intermediate example given its relatively high number of designated conservation areas (around 78,000) covering about 75% of the state. As part of the island of Great Britain, Scotland is surrounded by the Atlantic Ocean to the north and west, the North Sea to the northeast and the Irish Sea to the south. With a population density of about 68 people per km^2, most of Scotland's population is concentrated in the so-called Central Belt in the Scottish Lowlands – a plain located between the Scottish Highlands and the Southern Uplands.

3.2. Regional naturalness index maps

The NI maps produced for the three study areas are depicted in Fig. 5. For sake of comparison, we also provide the maps from two similar products, namely the Human Footprint (HF) and Human Modification (HM) in Fig. 6. In addition, the histograms of the NI values for the study areas are presented in Fig. 7. The differences between Bavaria, Lapland, and Scotland become immediately apparent: While Bavaria mostly exhibits NI values in the medium range, with a few places of higher NI values in the mountainous regions located in the southern, eastern and northwestern part of the state, Lapland shows the highest average NI score with a map that is mostly "green" – apart from the direct surroundings of the capital city of Rovaniemi and the coastal city of Kemi. Scotland, as expected, is placed between Bavaria and Lapland in terms of the average NI value. While large parts of the region are determined to be more natural than most parts of Bavaria, the afore-mentioned Central Belt is clearly depicted by low NI values in the map.

Fig. 8 aggregates the NI results over the three study regions in order to compare the average NI values between the overall landscape, urban areas, and different kinds of protected areas according to the International Union for the Conservation of Nature (IUCN):

- Category Ia refers to "Strict Nature Reserves", which are strictly protected areas designated to protect biodiversity by strictly controlling and limiting human impact.
- Category Ib refers to "Wilderness Areas", which are usually large in area and widely unmodified without significant human habitation.
- Category II finally defines "National Parks", which commonly are large (near) natural areas set aside to protect large-scale ecological processes and ecosystem characteristics. In contrast to the other two categories, human visitation is allowed and not uncommon.

The fact that the average NI values of those protected categories in the three study areas used in this paper are significantly larger than the average NI values of urban areas and even of the complete land surface of those areas confirms that the NI can indeed be used to distinguish more natural from less natural areas.

4. Discussion

As the results for the three study areas show, our approach allows the fully automatic generation of naturalness maps for extended regions. As Figs. 5–7 illustrate, a reasonable metric is produced, which indeed contains higher naturalness values for strongly protected conservation areas and lower values for the remaining areas, in particular urban areas. Similar to Fig. 6 but on a more detailed scale, Fig. 9 allows us to compare our new, high-resolution naturalness maps to state-of-the-art map products, i.e. the human footprint map and the human modification map, both in inverted form. In this zoom level, the better resolution of our new product can clearly be seen. This holds in particular for the Clyde Valley Woodlands National Nature Reserve shown in the top row of Fig. 9: While HF and HM would not allow to identify this small protected area at all due to their low resolutions, in our NI map the reserve can clearly be identified. Besides, some parts of the landscape adjacent to the reserve are identified as more natural than the surroundings, which could be used by local stakeholders as a starting point to discuss issues such as a potential extension of the reserve. Of course, it has to be noted that this statement holds only from a technical point of view, while the establishment or extension of protected areas to a large part is of course a political issue, which cannot be addressed by the presented methodology. While the second example – the Cairngorms National Park shown in the second row of Fig. 9 – is less obvious, also here the higher resolution of our approach is clearly visible. A comparison to the HF map confirms a general agreement of both measures, especially considering the less natural areas to the northwest of the park.

Although the approach described in this paper allows automatic generation of high-resolution land naturalness maps, there are a few limitations worth mentioning:

- Relying on OSM data for accessibility analysis has the disadvantage of using a non-homogenous dataset, varying in its completeness and accuracy. Besides, there is not yet an established, seamless workflow to import OSM data into Google Earth Engine.
- Some of the input datasets still are only provided with a resolution worse than our target resolution of 10 m per pixel (e.g. nighttime lights or population density data). It is expected that new products with improved resolution will further enhance the quality of our mapping results.
- Although we have followed the rationales of future work on human influence/modification/footprint and have defined naturalness as the opposite of those phenomena, naturalness is still a not physically measurable entity. Our work should thus be seen merely as a technical solution providing a sound, objective mapping product to domain experts (e.g. conservationists), who are invited to interpret them for further perusal.

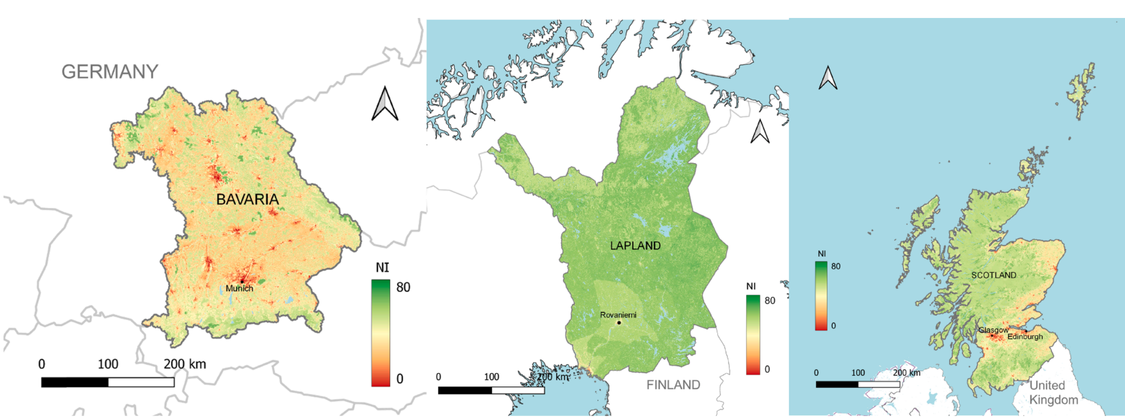

Fig. 5. The NI maps of Bavaria, Lapland, and Scotland produced with the method proposed in this article.

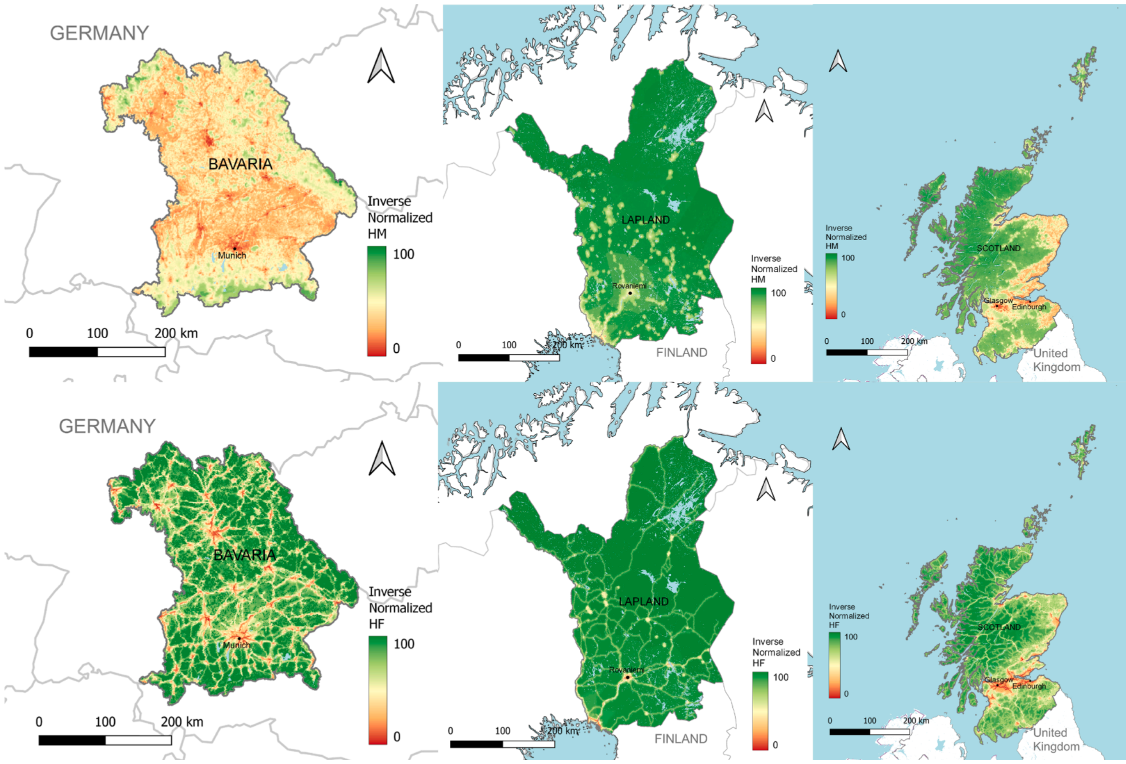

Fig. 6. Inverted Human Modification (HM, top row) and Human Footprint (HF, bottom row) maps for Bavaria, Lapland, and Scotland. A visual comparison to the NI maps depicted in Fig. 5 reveals a general agreement, although the HF seems to put a much stronger focus on trafficways, while both HM and HF seem to exaggerate the naturalness of the land occasionally.

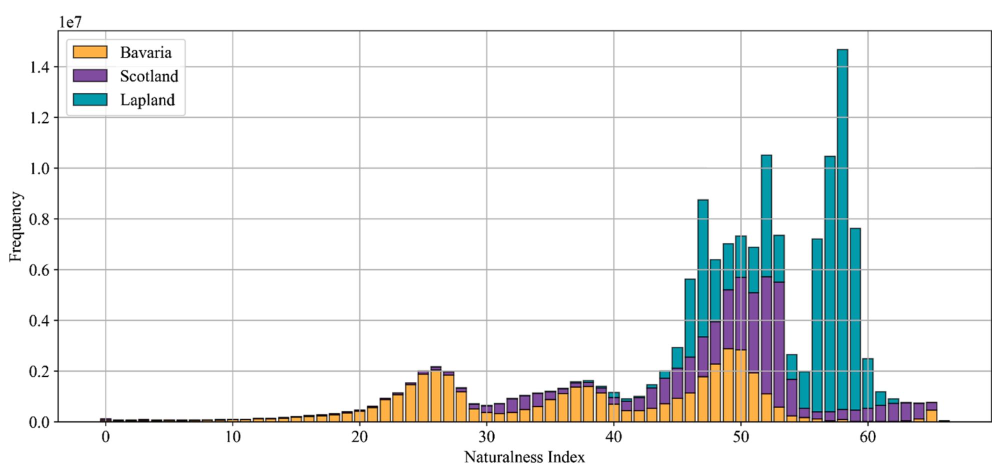

Fig. 7. Histogram of the NI values for the study areas. While the NI values for Bavaria are relatively spread out, the NI values for both Scotland and Lapland are peaking at higher levels.

5. Summary & conclusion

In this paper, we have presented the Naturalness Index as a new, high-resolution mapping of land naturalness (defined as the absence of human influence) on a regional scale. Its implementation in the cloud-computing environment of Google Earth Engine, and exploiting freely available, recent, and high-resolution geodata sources, allows an automated production of naturalness maps for extended land regions. Using the presented approach, we created example NI maps for three European study areas with different characteristics: Bavaria, Lapland, and Scotland. A detailed analysis of the resulting maps, including a comparison to existing state-of-the-art products, confirms the usefulness of the NI approach – in particular if a fine-grained, regional analysis is required. We believe that high-resolution NI maps can be used to provide relevant information to regional conservation stakeholders, e.g. in the context of debates about the establishment of new protected areas.

CRediT authorship contribution statement

Burak Ekim: Software, Validation, Formal analysis, Investigation, Writing – review & editing, Visualization. **Zeyu Dong:** Methodology, Software, Validation, Formal analysis, Investigation, Data curation, Writing – original draft, Visualization. **Dmitry Rashkovetsky:** Methodology, Software, Data curation, Writing – review & editing. **Michael Schmitt:** Conceptualization, Methodology, Resources, Writing – original draft, Writing – review & editing, Supervision, Project

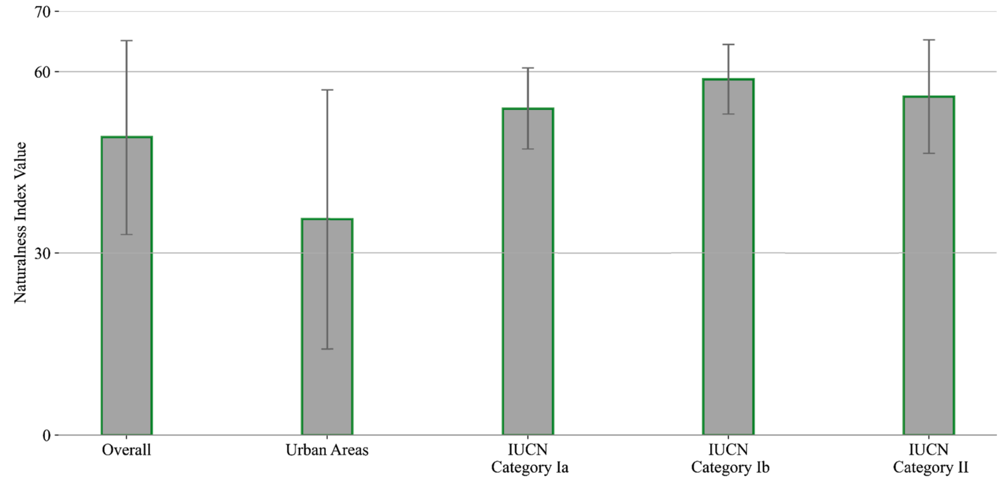

Fig. 8. Comparison of the average NI values for different area categories. The fact that protected conservation areas exhibit higher NI values than, e.g., urban areas, is clearly visible. This confirms the usefulness of the NI for a distinction of less natural and more natural areas.

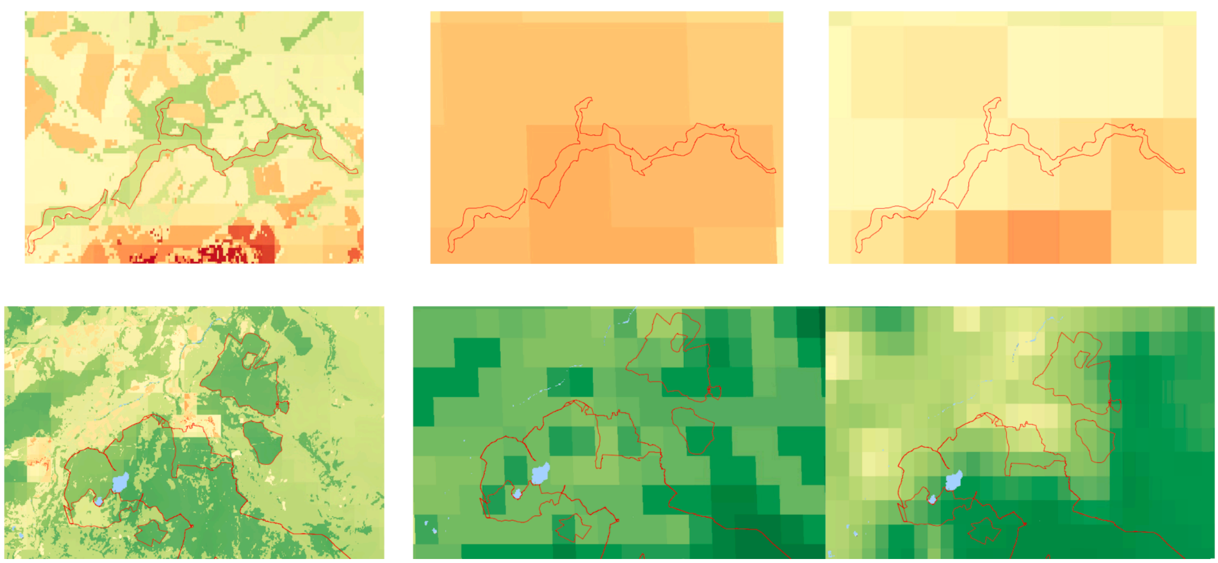

Fig. 9. Close-look, from left to right: NI, HM, and HF values. Red polygons indicate IUCN designated areas. First row: Clyde Valley Woodlands National Nature Reserve, Scotland. Second row: Cairngorms National Park, Scotland.

administration, Funding acquisition.

Declaration of Competing Interest

The authors declare that they have no known competing financial interests or personal relationships that could have appeared to influence the work reported in this paper.

Acknowledgments

This work was supported by the German Research Foundation (DFG project MapInWild, grant SCHM 3322/4-1), by the Stifterverband (Open Data Impact Award) and by the open-access publication fund of the Bundeswehr University Munich.

References

Allan, J.R., Venter, O., Watson, J.E.M., 2017. Temporally intercomparable maps of terrestrial wilderness and the Last of the Wild. Sci. Data 4 (1), 170187.

Balmford, A., Bruner, A., Cooper, P., Costanza, R., Farber, S., Green, R.E., Jenkins, M., Jefferiss, P., Jessamy, V., Madden, J., Munro, K., Myers, N., Naeem, S., Paavola, J., Rayment, M., Rosendo, S., Roughgarden, J., Trumper, K., Turner, R.K., 2002. Economic reasons for conserving wild nature. Science 297 (5583), 950–953.

Brackhane, S., Klein, B., Reif, A., Schmitt, C.B., 2021. Implementing the 2% wilderness goal in Germany – the national natural heritage site Rechlin as a case study. J. Nature Conserv. 64, 126067.

Cao, Y., Carver, S., Yang, R., 2019. Mapping wilderness in China: comparing and integrating Boolean and WLC approaches. Landscape Urban Plann. 192, 103636.

Carver, S., Fritz, S., 2016. Mapping Wilderness: Concepts, Techniques and Applications. Dordrecht: Springer.

Carver, S., Tricker, J., Landres, P., 2013. Keeping it wild: mapping wilderness character in the United States. J. Environ. Manage. 131, 239–255.

Cincotta, R.P., Wisnewski, J., Engelman, R., 2000. Human population in the biodiversity hotspots. Nature 404 (6781), 990–992.

Fritz, S., Carver, S., See, L., 2000. New GIS approaches to wild land mapping in Europe. In: USDA Forest Service Proceedings RMRS-P-15-VOL-2, pp. 120–127.

Gorelick, N., Hancher, M., Dixon, M., Ilyushchenko, S., Thau, D., Moore, R., 2017. Google earth engine: planetary-scale geospatial analysis for everyone. Remote Sens. Environ. 202, 18–27.

Haklay, M., 2010. How good is volunteered geographical information? A comparative study of OpenStreetMap and ordnance survey datasets. Environ. Plan. B: Plan. Design 37 (4), 682–703.

Hansen, M.C., Potapov, P.V., Moore, R., Hancher, M., Turubanova, S.A., Tyukavina, A., Thau, D., Stehman, S.V., Goetz, S.J., Loveland, T.R., Kommareddy, A., Egorov, A., Chini, L., Justice, C.O., Townshend, J.R.G., 2013. High-resolution global maps of 21st-century forest cover change. Science 342 (6160), 850–853.

Kennedy, C.M., Oakleaf, J.R., Theobald, D.M., Baruch-Mordo, S., Kiesecker, J., 2019. Managing the middle: a shift in conservation priorities based on the global human modification gradient. Glob. Change Biol. 25 (3), 811–826.

Ma, S., Long, Y., 2020. Mapping potential wilderness in China with location-based services data. Appl. Spatial Anal. Policy 13 (1), 69–89.

Potapov, P., Hansen, M.C., Laestadius, L., Turubanova, S., Yaroshenko, A., Thies, C., Smith, W., Zhuravleva, I., Komarova, A., Minnemeyer, S., Esipova, E., 2017. The last frontiers of wilderness: tracking loss of intact forest landscapes from 2000 to 2013. Sci. Adv. 3 (1), e1600821.

Sanderson, E.W., Jaiteh, M., Levy, M.A., Redford, K.H., Wannebo, A.V., Woolmer, G., 2002. The human footprint and the last of the wild. Bioscience 52 (10), 891–904.

Tobler, W., 1993. Three presentations on geographical analysis and modeling: non-isotropic geographic modeling speculations on the geometry of geography global spatial analysis. National Center for Geographic Information and Analysis: Technical Report 93-1.

Venter, O., Sanderson, E.W., Magrach, A., Allan, J.R., Beher, J., Jones, K.R., Possingham, H.P., Laurance, W.F., Wood, P., Fekete, B.M., Levy, M.A., Watson, J.E. M., 2016. Global terrestrial human footprint maps for 1993 and 2009. Sci. Data 3 (1), 160067.

World Health Organization, 2020. WHO Manifesto for a healthy recovery from COVID-19. Available online at: https://www.who.int/docs/default-source/climate-change/who-manifesto-for-a-healthy-and-green-post-covid-recovery.pdf.

Zanaga, D., Van De Kerchove, R., De Keersmaecker, W., Souverijns, N., Brockmann, C., Quast, R., Wevers, J., Grosu, A., Paccini, A., Vergnaud, S., Cartus, O., Santoro, M., Fritz, S., Georgieva, I., Lesiv, M., Carter, S., Herold, M., Li, Linlin, Tsendbazar, N.E., Ramoino, F., Arino, O., 2021. ESA WorldCover 10 m 2020 v100.